Noname manuscript No.
(will be inserted by the editor)

Transmission of a Detonation across a Density Interface

K.C. Tang Yuk · X.C. Mi · J.H.S. Lee · H.D. Ng

Received: date / Accepted: date

Abstract The present study investigates the transmission of a detonation wave across a density interface. The problem is first studied theoretically considering an incident CJ detonation wave, neglecting its detailed reaction-zone structure. It is found that, if there is a density decrease at the interface, a transmitted strong detonation wave and a reflected expansion wave would be formed; if there is a density increase, one would obtain a transmitted CJ detonation wave followed by an expansion wave and a reflected shock wave. Numerical simulations are then performed considering that the incident detonation has the ZND reaction-zone structure. The transient process that occurs subsequently to the detonation-interface interaction has been captured by the simulations. The effects of the magnitude of density change across the interface and different reaction kinetics (i.e., single-step Arrhenius kinetics vs. two-step induction-reaction kinetics) on the dynamics of the transmission process are explored. After the transient relaxation process, the transmitted waves reach the final state in the new medium. For the cases with two-step induction-reaction kinetics, the transmitted wave fails to evolve to a steady detonation wave if the magnitude of density increase is greater than a critical value. For the cases wherein the transmitted wave can evolve to a steady detonation, the numerical results for both reaction models give final propagation states that agree with the theoretical solutions.

K.C. Tang Yuk, X.C. Mi, and J.H.S. Lee
Department of Mechanical Engineering, McGill University, Montreal, Quebec, Canada H3A 0C3
E-mail: kelsey.tangyuk@mail.mcgill.ca

H.D. Ng
Department of Mechanical and Industrial Engineering, Concordia University, Montreal, Quebec, Canada H4B 1R6
E-mail: hoing@encs.concordia.ca

Keywords Detonation · interface · transmission · contact surface · density change · inhomogeneous · relaxation process

1 Introduction

Inhomogeneities are inevitable in practical explosive mixtures. For example, in accidentally released clouds of combustible fuel, nonuniformities in chemical composition are commonly present. Due to the temperature difference between the released fuel clouds and the surroundings (e.g., ground, ambient atmosphere), temperature, and hence, density gradients may be formed within the explosive mixture. Furthermore, in propulsion applications of detonation waves, such as Rotating Detonation Engines (RDEs), inhomogeneities in the form of interfaces and concentration gradients are present in the combustion chamber due to discretely located injection of reactants. It is therefore of practical importance to examine how detonation waves interact with inhomogeneities.

The response of gaseous detonation waves to inhomogeneities is complicated by the fact that the detonation wave structure is transient and spatially nonuniform. As such, a detonation wave complex propagates in a nonuniform medium, its entire structure is subjected to perturbations due to the presence of inhomogeneities. The wave propagation thus undergoes an unsteady relaxation process in response to these perturbations. Probing the dynamics underlying this relaxation process may reveal some insights into the intrinsic propagation mechanism of detonation waves.

Detonations propagating in reactive mixtures with embedded nonuniformities have been experimentally implemented in various ways. Bjerketvedt *et al.* studied a

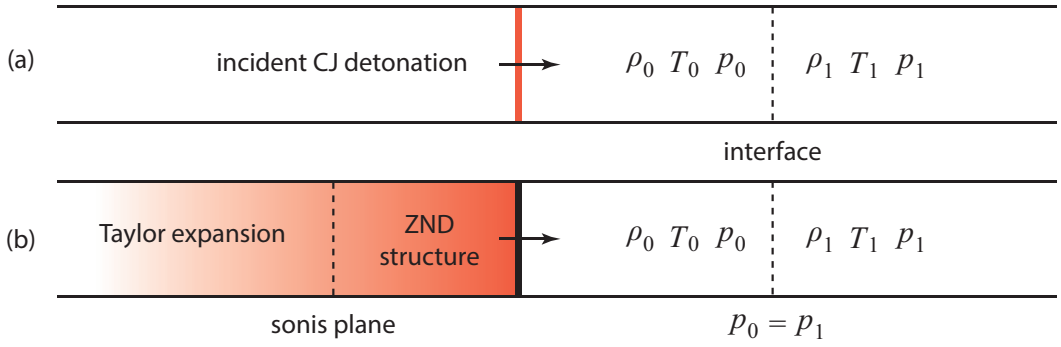

Fig. 1 Problem schematic: (a) A simplified model considering an incident CJ detonation wave without considering its detailed structure and (b) a model considering an incident detonation wave with the ZND structure.

detonation wave propagating across an inert gap of air, showing that whether a detonation can be re-initiated downstream from the gap depends on the gap width and the properties of the reactive mixtures. [1] In some studies, a reactive medium with gradual changes in chemical composition, e.g., a gradient in fuel concentration, was created via diffusion of the reactants in a vertical tube (or channel). [2,3] The propagation behavior of the detonation wave at chemical composition gradients has been recorded as gradual changes in the propagation velocity and detonation cell size. [2,3] It is important to note that, in both of the above-mentioned experimental scenarios, a finite length scale of the inhomogeneity, i.e., the width of the inert gap or the length throughout which the gradient is spread, has been introduced into the system. This length scale in addition to the intrinsic length scales of the detonation waves further complicates the underlying dynamics. Hence, introducing an inhomogeneity of a negligible length comparing the thickness of detonation structure might be a more easily diagnosable set-up to study this problem. Thus, the interest in the transmission of a detonation wave across an interface–over which the thermodynamic, flow, and chemical properties change abruptly–is motivated.

A benchmark scenario for examining the transmission of a detonation wave across a discontinuity is the transmission from a reactive mixture into an inert medium, i.e., detonation-to-shock transmission. Some experimental studies on this problem have shown that the properties of the transmitted shock wave well agree with those predicted by the theoretical models. [2,4,5]. Studies on the transmission of a detonation wave across an interface that separates two reactive mixtures with different properties was first conducted by Strehlow *et al.* [6], and later, by Kuznetsov *et al.* [7,8] and Li *et al.* [9, 10]. In these experimental set-ups, the two mixtures were initially separated by a thin diaphragm or a sliding valve. Rupture of the diaphragm and opening of the valve likely disturb the interface, introducing considerable uncertainties to the experimentally recorded wave evolution downstream from the interface. Thus, in an attempt to create an abrupt, planar discontinuity, the head-on collision of a detonation wave with a weak shock wave was studied [11,12]. In these cases, since an incident detonation wave is subjected to an abrupt change in density, pressure, temperature, and flow velocity, it is rather difficult to diagnose the mechanisms underlying the relaxation behavior of the transmitted detonation wave into the shocked region.

Concerning the difficulties in devising experiments to examine the transmission of a detonation wave across an undisturbed interface, it is perhaps more convenient to approach this problem via theoretical analysis and computational simulations. In the current study, a detonation wave subjected to an abrupt change in density and temperature is considered in a one-dimensional system with initially uniform pressure and stationary flow. The objective of this study is to probe the response of the detonation wave to various magnitudes of density increase and decrease across the interface. To this end, two different models are used in this study: (1) A simple model with an incident Chapman-Jouguet (CJ) detonation wave wherein the reaction zone structure of the detonation is neglected (as shown in Fig. 1(a)); (2) a more complex model considering an incident detonation wave with the corresponding Zel'dovich-von Neumann-Döring (ZND) reaction-zone structure (as shown in Fig. 1(b)). The simple model with an incident CJ wave can be analytically solved to obtain the steady-state properties of the transmitted detonation. To examine the relaxation process, the second model considering the ZND wave profile needs to be solved numerically. In this paper, these two models are referred to as the *CJ-wave model* and the *ZND-wave model*, respectively.

This paper is organized as follows. Section 2 is focused on the CJ-wave model. The analytic results of the transmitted detonation are presented in this section. The ZND-wave model is shown in Sect. 3. The numer-

ical results of the relaxation process of the transmitted detonation are presented in this section. In Sect. 4, the simulation results of the steady-state velocity of the transmitted detonation are compared with the corresponding theoretical results. The findings of this study are summarized in the Conclusion (Sect. 5).

2 The CJ-wave model

This model considers a one-dimensional system with calorically ideal gas. An incident detonation wave propagates rightward and transmits across an interface over which initial density and temperature changes abruptly while maintaining the same pressure. The flow in the system is initially stationary. The adiabatic index γ is the same on both sides of the interface. If the incident detonation wave is considered as the CJ solution (as shown in Fig. 1(a)), without taking the detailed reaction-zone structure into account, then a standard wave interaction analysis of the transmission problem can be carried out. The x-t diagram of the wave process is shown in Fig. 2. The flow behind the incident detonation (in Region 2 shown in Fig. 2) is assumed to be uniform. This assumption is valid in the case where the back boundary of the system is very far downstream from the CJ wave so that the trailing Taylor rarefaction wave has very shallow gradients.

Across the interface, the initial density either increases ($\rho_1 > \rho_0$) or decreases ($\rho_1 < \rho_0$). While maintaining the same initial pressure across the interface, i.e., $p_0 = p_1$, the initial temperature downstream from the interface T_1 must be varied reciprocally to the change in density as follows,

$$\frac{\rho_1}{\rho_0} = \frac{T_0}{T_1} \tag{1}$$

The change in the acoustic impedance $z = \rho c = \rho\sqrt{RT}$ across the interface is thus related to the change in density as follows,

$$\frac{z_1}{z_0} = \frac{\rho_1\sqrt{RT_1}}{\rho_0\sqrt{RT_0}} = \sqrt{\frac{\rho_1}{\rho_0}} \tag{2}$$

Equation 2 shows that, as density increases across the interface, acoustic impedance increases; as density decreases, acoustic impedance decreases. For this problem, it is thus valid to consider the density ratio at the interface as an indicator of the corresponding acoustic-impedance ratio. Although shock-impedance ratio should be considered to predict shock-interface interactions, according to the analysis performed by Haselbacher [13], for the case wherein γ is the same on both sides of the interface, considering acoustic-impedance ratio is sufficiently accurate for making this prediction. Therefore,

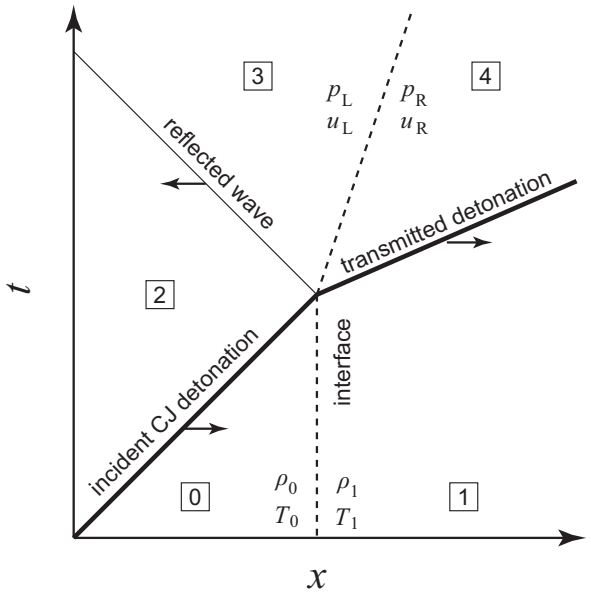

Fig. 2 x-t diagram showing a CJ detonation wave transmitting across a density interface.

all the results presented in this paper are parametrized by the magnitude of density increase and decrease across the interface, which is reported as $\Delta\rho = (\rho_1 - \rho_0)/\rho_0$ in percentage.

2.1 Theoretical analysis

The problem is defined for a given incident detonation Mach number, $M_{\mathrm{D,i}} = M_{\mathrm{CJ,i}}$, and properties on each side of the interface. As the incident detonation reaches the interface, as shown in Fig. 2, a reflected wave and a transmitted detonation are formed. The reflected wave can be a shock wave or a rarefaction wave depending on the nature of the acoustic impedance mismatch at the interface. The transmitted detonation can be the strong, weak, or CJ detonation solution. The weak detonation solution can be eliminated in general. [14,15]

If the transmitted detonation wave is the strong solution, the product flow (in Region 4 shown in Fig. 2) is subsonic and uniform up to the contact surface. If the transmitted detonation wave is CJ, then the flow can either be uniform up until the contact surface or there can be an expansion wave trailing behind the transmitted detonation wave. Thus, there can be either a transmitted strong or CJ detonation wave with uniform flow behind it or a transmitted CJ detonation wave with an expansion wave behind it. Thus, there are four possible configurations of the transmitted detonation and the reflected wave as summarized in Table 1.

Table 1 Possible wave configurations

case	reflected wave	transmitted detonation
1	shock wave	strong or CJ with uniform flow
2	shock wave	CJ with expansion wave
3	expansion wave	strong or CJ with uniform flow
4	expansion wave	CJ with expansion wave

For the incident and transmitted detonation waves, the relationships across the wave are given as follows,

$$\begin{aligned} \frac{p_{\mathrm{d}+}}{p_-} &= \frac{\gamma+\eta\pm\gamma s}{\eta(1+\gamma)} \\ \frac{\rho_{\mathrm{d}+}}{\rho_-} &= \frac{\gamma+1}{(\gamma+\eta\mp s)} = \frac{D}{D-u_+} \\ M_{\mathrm{D}} &= \frac{D}{c_-} \end{aligned} \tag{3}$$

where

$$\begin{aligned} s &= \pm\sqrt{(1-\eta_{\mathrm{D}})^2 - K\eta_{\mathrm{D}}} \\ \eta_{\mathrm{D}} &= \frac{1}{{M_{\mathrm{D}}}^2} = (1+\frac{K}{2}) - \sqrt{K(1+\frac{K}{4})} \\ K &= 2(\gamma^2-1)\frac{Q}{\gamma p_- v_-} \end{aligned} \tag{4}$$

Variables p, ρ, v, u, and c are pressure, density, specific volume, particle velocity, and the speed of sound respectively, M_D is the Mach number of the detonation wave, D is its velocity and Q is the chemical heat released per unit mass in the reaction. In the above equations, the "+" and "−" indicate the properties behind and in front of the wave, respectively. The "D" subscript indicates that these flow values are at the end of the detonation reaction zone. In this way, one can distinguish the state "D+" at the exit of a detonation wave and the state "+" behind a shock wave. The strong and weak detonation solutions are associated with the positive and negative values of s in Eq. 4, respectively. If $s = 0$, the CJ solution is obtained.

In the reflected wave is a shock, the pressure and flow velocity behind the shock wave can be obtained via the Rankine-Hugoniot relations as follows,

$$\begin{aligned} \frac{p_+}{p_-} &= \frac{2\gamma {M_{\mathrm{s}}}^2 - (\gamma-1)}{\gamma+1} \\ \frac{u_+ - u_-}{c_-} &= \frac{2({M_{\mathrm{s}}}^2-1)}{(\gamma+1)M_{\mathrm{s}}} \end{aligned} \tag{5}$$

where M_{s} is the shock wave Mach number and c is the sound speed.

For an expansion wave–either reflected from the interface or trailing a transmitted CJ detonation–the change in pressure and flow velocity can be obtained via the isentropic relations and the characteristic equations (i.e., constant Riemann invariant along a characteristic), respectively, as follows,

$$\begin{aligned} \frac{c_+}{c_-} &= (\frac{p_+}{p_-})^{\frac{\gamma-1}{2\gamma}} \\ u_+ + \frac{2}{\gamma-1}c_+ &= u_- + \frac{2}{\gamma-1}c_- \end{aligned} \tag{6}$$

With these relations for detonation, shock, and expansion waves, knowing the Mach number of the incident CJ detonation $M_{\mathrm{CJ,i}}$ and the initial properties across the interface, the configuration of the transmitted detonation and the reflected wave with unique properties can be solved by applying mechanical equilibrium conditions at the advected contact surface, i.e., $p_{\mathrm{L}} = p_{\mathrm{R}}$ and $u_{\mathrm{L}} = u_{\mathrm{R}}$.

2.2 Theoretical solutions

The problem was solved for a range of incident detonation Mach numbers (3.0 to 7.3) with a range of density changes (-50% to +50%). The solution wave pattern was found to depend on whether there is a density increase or decrease. For a density decrease (and temperature increase), a transmitted strong detonation and a reflected expansion wave are obtained. This resulting wave configuration corresponds to Case 3 in Table 1 and is depicted in Fig. 3(a). For a density increase (and temperature increase), a transmitted CJ detonation with an expansion wave and a reflected shock wave are obtained. This resulting wave configuration corresponds to Case 2 in Table 1 and is depicted in Fig. 3(b). The detailed analytic solutions for these two cases can be found in the Appendix.

The degree of overdrive of the transmitted detonation is defined as $f = D_{\mathrm{t}}^2/D_{\mathrm{CJ}}^2$ where D_{t} is the speed of the transmitted detonation and D_{CJ} the CJ detonation in the downstream medium (on the right of the interface). This is plotted against the percentage density change for selected incident detonation Mach numbers, $M_{\mathrm{D,i}} = M_{\mathrm{CJ,i}}$ in Fig. 4. For all cases, the transmitted detonation is strong ($f > 1$) for a density decrease and CJ ($f = 1$) for a density increase. The degree of overdrive f increases with increasing magnitude of density decrease and increasing $M_{\mathrm{CJ,i}}$.

3 The ZND-wave model

In this model, the incident detonation wave has the ideal ZND reaction-zone structure. Transient response of the transmitted detonation can thus be captured via numerical simulations. The governing equations of this model and the numerical methodologies used to solve

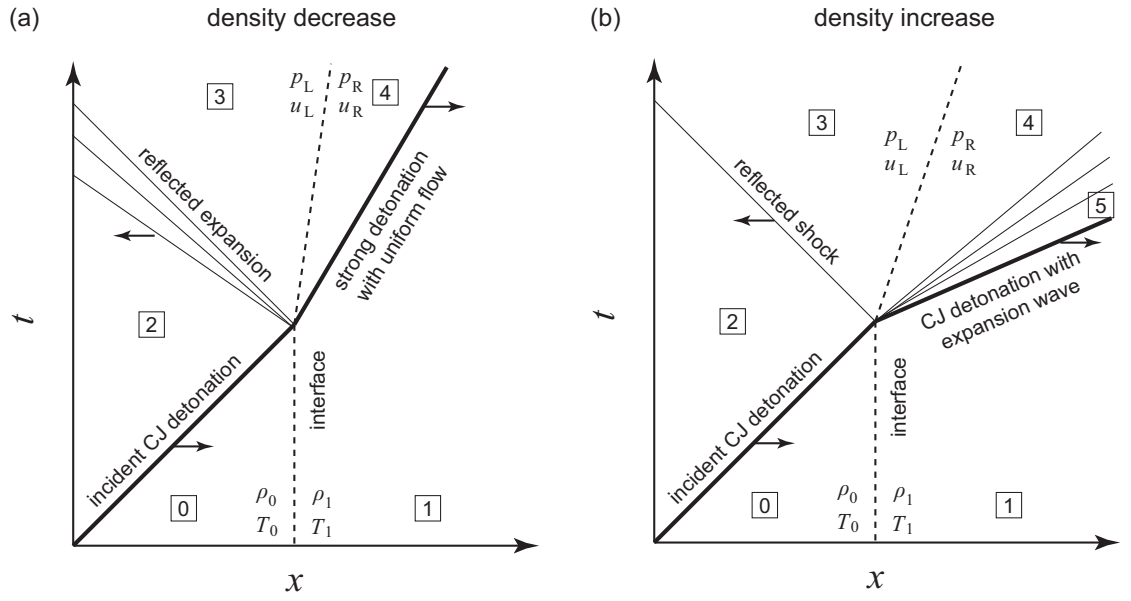

Fig. 3 x-t diagrams showing the resulting wave configurations for the cases with density (a) decrease and (b) increase across the interface.

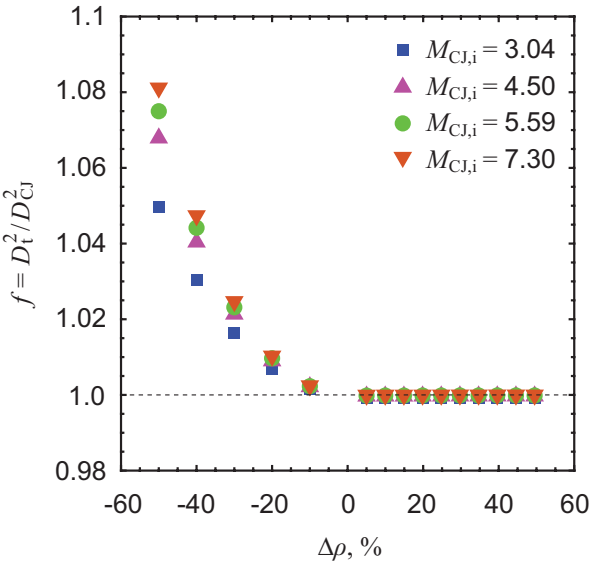

Fig. 4 Degree of overdriven of the transmitted detonation with respect to the local CJ velocity ($f = {D_t}^2/{D_{CJ}}^2$) as a function of the percentage density change across the interface for various incident Mach numbers $M_{CJ,i}$

these equations are presented in Sect. 3.1 and 3.2, respectively. The simulation results of the relaxation process are shown in Sect. 3.3 where the effects of the magnitude of density decrease and increase and various reaction kinetics are explored.

3.1 Governing Equations

This model is governed by the one-dimensional, reactive Euler equations:

$$\frac{\partial \mathbf{U}}{\partial t} + \frac{\partial \mathbf{F}(\mathbf{U})}{\partial x} = \mathbf{S}(\mathbf{U}) \tag{7}$$

$$\mathbf{U} = \begin{bmatrix} \rho \\ \rho u \\ E \\ \rho\lambda \end{bmatrix}, \mathbf{F}(\mathbf{U}) = \begin{bmatrix} \rho u \\ \rho u^2 + p \\ (E+p)u \\ \rho u \lambda \end{bmatrix}, \mathbf{S}(\mathbf{U}) = \begin{bmatrix} 0 \\ 0 \\ 0 \\ \dot{\omega} \end{bmatrix} \tag{8}$$

where e is the total energy per unit mass given by,

$$e = \frac{p}{(\gamma-1)\rho} + \frac{u^2}{2} + \lambda Q \tag{9}$$

The variables in the governing equations are nondimensionalized with respect to the initial state 0 upstream from (i.e., on the left side of) the interface face.

The governing equations are coupled with a chemical kinetic law for the reaction rate, $\dot{\omega}$. The reaction progress variable is denoted as λ, where $\lambda = 0$ for reactants and $\lambda = 1$ for products. In this study, two different reaction rate laws were considered, i.e., single-step kinetics and two-step induction-reaction kinetics.

The simpler case is a single-step reaction law in the Arrhenius form as follows,

$$\frac{\partial(\rho\lambda)}{\partial t} = \dot{\omega} = k\rho(1-\lambda)\exp\left(\frac{-E_a}{T}\right) \tag{10}$$

where E_a is the activation energy and T is temperature. A pre-exponential constant for a given mixture k is used to define spatial and temporal scales.

A more realistic reaction model includes an induction zone. The reaction zone is modeled in the same way and the induction zone is also of an Arrhenius type as follows,

$$\begin{aligned}\frac{\partial(\rho\lambda)}{\partial t} &= \dot{\omega} = (1 - H(1-\xi))k_r\rho\lambda\exp\left(\frac{-E_r}{T}\right) \\ \frac{\partial(\rho\xi)}{\partial t} &= H(1-\xi)\rho k_i\exp\left[E_i\left(\frac{1}{T_+} - \frac{1}{T}\right)\right]\end{aligned} \tag{11}$$

$$H(1-\xi) = \begin{cases} 1 & \xi < 1 \\ 0 & \xi \geq 1 \end{cases} \tag{12}$$

where there is a reaction zone progress variable, λ and an induction zone progress variable, ξ. They increase from 0 at the beginning of their respective zones to 1 at the end. There are also two activation energies and pre-exponential factors, E_i and k_i for the induction zone and E_r and k_r for the reaction zone. T_+ is the temperature at the shocked state. Parameters for specifying activation energy ϵ_i and ϵ_r are defined to be E_i/μ and E_r/μ, respectively, where μ is the temperature jump across the leading shock of the detonation.

3.2 Numerical methodology

The computational domain was defined on a one-dimensional, uniform Cartesian grid. Transmissive boundary conditions were applied on the left and right of this domain. The governing equations are numerically integrated using the method of fractional steps and two second-order finite volume schemes. These are the slope-limited centered (SLIC) and the upwind weighted averaged flux (WAF) schemes. [16]. The upwind WAF scheme with an exact Riemann solver was used with the single-step Arrhenius kinetic model. The SLIC scheme was used with the two-step induction-reaction kinetic model. Validations of these codes in gaseous detonation simulations can be found in Refs. [17,18].

The resolution was assessed by comparing the computational grid size to the characteristic length of the reaction zone coupled to the leading shock front. For the single-step Arrhenius reaction model, the characteristic length scale corresponds to the half reaction zone length of the initial, steady ZND wave. For the two-step induction-reaction kinetic model, the initial, steady induction zone length is used as the characteristic length scale. A resolution of 100 grid points per characteristic length of the reaction zone was used, as verified in previous convergence studies [17,18]. The pre-exponential factors were scaled such that the characteristic lengths of the reaction zone were unity. For the two-step induction-reaction kinetic model, k_i is set to be the particle velocity behind the shock front in the shock-fixed frame, $u_{D,+}$.

A rightward-propagating detonation was initialized by imposing the steady ZND wave solution on the grid near the left end of the domain. The leading shock front is initially 10 characteristic reaction-zone lengths away from the left boundary. The ZND solution was obtained by integrating the governing equations for a steady state, i.e., Eq. 7 with $\partial\mathbf{U}/\partial\mathbf{t} = \mathbf{0}$, considering the Mach number of the leading shock is the M_{CJ}. The ODELS solver included in the the FORTRAN library ODEPACK was used to perform this numerical integration. The Backward Differentiation Formula (BDF) methods are implemented in this solver to tackle stiff equations. [19] The detonation was allowed to propagate over a sufficient distance (at least 400 characteristic reaction-zone lengths of the incident ZND detonation) before the interface was encountered in order to eliminate influences from the rear boundary of the system.

3.3 Results

Since the incident detonation has a reaction zone of finite thickness, the final state cannot be achieved instantaneously downstream of the density interface. There is an unsteady period during which the detonation responds to the abrupt change in density. Subsequently, the detonation gradually relaxes to its final downstream state. Note that all the length scales reported in this section are normalized by δ the 90%-complete reaction zone length (where $\lambda = 0.9$) in the corresponding ZND solution. The x-coordinates are shifted so that the interface is initially located at $x/\delta = 0$. All the simulations presented in this section are for the cases with $Q = 50$ and $\gamma = 1.2$.

3.3.1 Dynamics of the relaxation process

In this subsection (Sect. 3.3.1), the transient dynamics of the relaxation process is first studied using the simpler reaction model, i.e., single-step Arrhenius kinetics with $E_a = 20$.

A sample case with a density decrease and temperature increase across the interface is first considered. In Fig. 5(a), pressure contours are plotted as an x-t diagram showing the evolution of the flow field in the course of a detonation wave with the ZND structure transmitting across the interface for the case with a

density decrease of $\Delta\rho = -25\%$. The contour lines of the absolute value of density gradient are plotted as thin gray curves in Fig. 5(a). On this x-t diagram, the transmitted detonation, advected contact surface, and reflected rarefaction wave can be identified. In the case with a density decrease (and temperature increase while maintaining the same pressure) over the interface, there is correspondingly a decrease in acoustic impedance. The leading shock wave encountering such an interface thus generates a reflected rarefaction wave and undergoes an abrupt decrease in shock pressure. [20]

In Fig. 5(b), the history of the leading shock pressure ratio p_+/p_0 is plotted as a function of the normalized leading shock position x_s/δ to show the full relaxation process of the transmitted detonation for the case with a density decrease of $\Delta\rho = -25\%$. The location of the interface is indicated by the thin dash line in Fig. 5(b). Immediately downstream from the interface, as expected on the basis of gasdynamic considerations, the shock pressure undergoes an abrupt decrease to about 80% of its its initial value, i.e., the von Neumann pressure of the incident detonation. This is followed by a rapid re-acceleration up to a distance of $x_s/\delta \approx 5$. Subsequently, at a location $x_s/\delta \approx 20$ downstream from the interface, the leading shock pressure decreases to be within 5% of the steady-state value.

A sample case with a density increase and temperature decrease across the interface is next considered. In Fig. 6(a), pressure contours are plotted as an x-t diagram showing the evolution of the flow field in the course of a detonation wave with the ZND structure transmitting across the interface for the case with a density increase of $\Delta\rho = +20\%$. The contour lines of the absolute value of density gradient are plotted as thin gray curves in Fig. 6(a). On this x-t diagram, the transmitted detonation, advected contact surface, and reflected shock wave can be identified. In the case with a density increase (and temperature decrease while maintaining the same pressure) over the interface, there is correspondingly an increase in acoustic impedance $z = \rho c = \rho\sqrt{RT}$. The leading shock wave encountering such an interface thus generates a reflected shock wave and undergoes an abrupt increase in shock pressure. [20]

In Fig. 6(b), the history of the leading shock pressure ratio p_+/p_0 is plotted as a function of the normalized leading shock position x_s/δ to show the full relaxation process of the transmitted detonation for the case with a density increase of $\Delta\rho = +20\%$. The location of the interface is indicated by the thin dash line in Fig. 6(b). Upon the detonation-interface interaction there is an abrupt increase of approximately 10% in the leading shock pressure ratio. This is followed by a decay to a minimum in the leading shock pressure at $x_s/\delta \approx 10$, which corresponds to a sub-CJ state of approximately 85% of the CJ detonation velocity of the gas downstream the interface. Subsequently, the wave accelerates and reaches a peak shock pressure of $p_+/p_0 \approx 59$ at $x_s \approx 30$. The leading shock pressure then gradually decreases. At a location $x_s/\delta \approx 37$ downstream from the interface, the leading shock pressure decreases to be within 5% of a steady-state value.

3.3.2 Effect of the magnitude of density decrease and increase $\Delta\rho$

In Fig. 7(a), the evolution histories of the leading shock pressure p_+/p_0 are plotted as functions of the normalized leading shock position x_s/δ for the cases with single-step Arrhenius kinetics ($E_a = 20$) and density decreases of -15%, -25% and -35%. As shown in Fig. 7(a), the relaxation processes for different magnitudes of density decrease are qualitatively similar, i.e., an abrupt decrease in shock pressure followed by an acceleration phase to reach a peak shock pressure, and then a relatively slow decay to a steady state. At the interface (indicated by the vertical dash line in Fig. 7(a)), the magnitude of the abrupt drop in shock pressure becomes greater for increasingly large density decrease. This trend is due to the fact that the magnitude of the decrease in acoustic impedance over the interface increases for greater magnitudes of density decrease. Further, it can be noticed in Fig. 7(a) that, as the magnitude of density decrease increases, the subsequent increase in shock pressure becomes steeper, and the peak shock pressure decreases. Recall that, for a greater magnitude of density decrease, the increase in temperature is greater, resulting in a greater shock temperature of the transmitted detonation after the interface, $T_{+,t}$. Since the reaction rate is an exponential function of temperature (Eq. 10), this greater shock temperature leads to a more rapid reaction rate, and thus, a steeper increase in shock pressure of the transmitted detonation.

In Fig. 7(b), the evolution histories of the leading shock pressure p_+/p_0 are plotted as functions of the normalized leading shock position x_s/δ for the cases with single-step Arrhenius kinetics ($E_a = 20$) and density increases of $+10\%$, $+20\%$, and $+30\%$. At the interface, as shown in Fig. 7(b), the abrupt increase in shock pressure is more pronounced for increasing greater magnitudes of density increase over the interface. This trend can again be explained on the basis of gasdynamic considerations: the magnitude of the increase in acoustic impedance over the interface increases for greater magnitudes of density increase. For increasingly greater magnitude of density increase, the downstream temper-

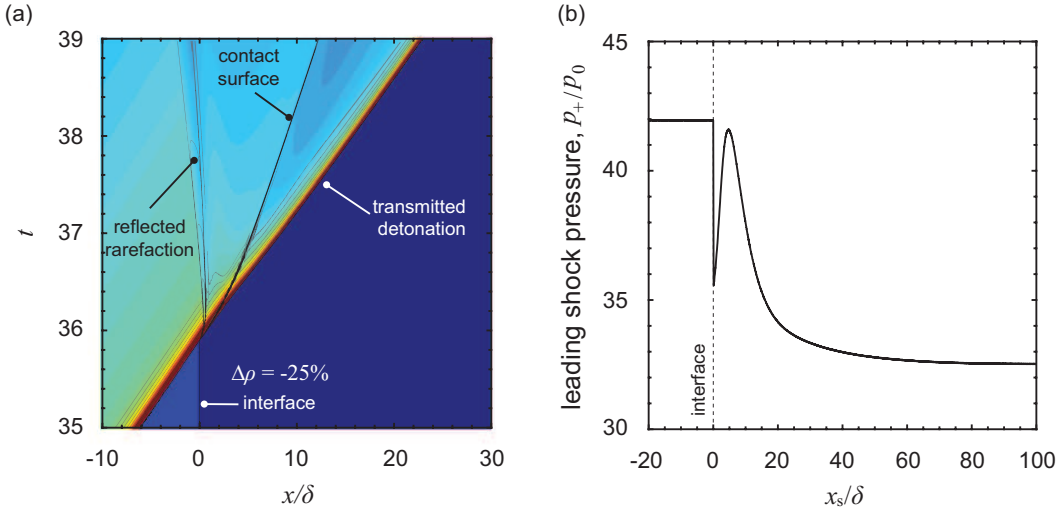

Fig. 5 Relaxation process for density decrease $\Delta\rho = -25\%$ and single-step Arrhenius kinetics with $E_a = 20$, $Q = 50$ and $\gamma = 1.2$: (a) The x-t diagrams showing the density contour with various wave features; (b) history of the leading shock pressure p_+/p_0 as a function of the leading shock position x_s normalized by the 90%-reaction-zone length δ.

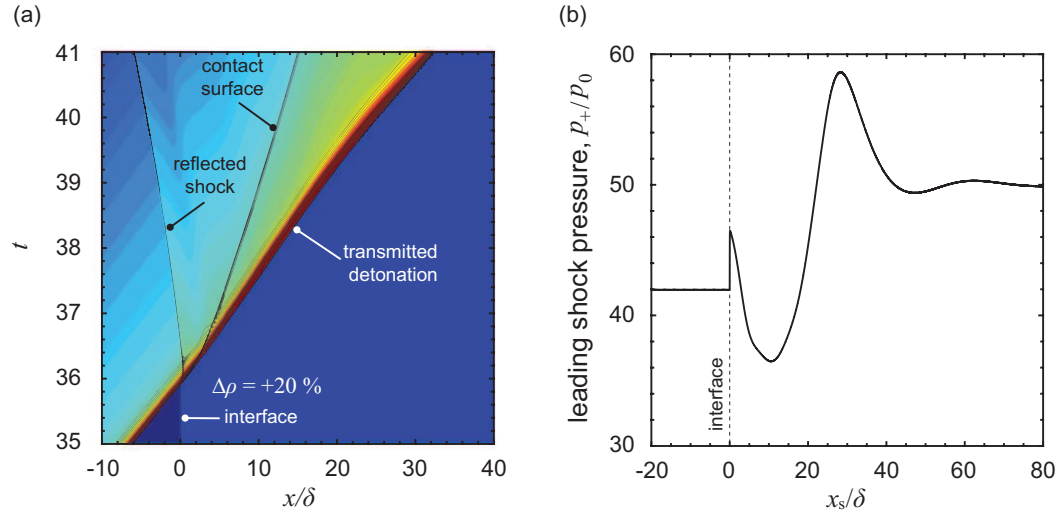

Fig. 6 Relaxation process for density increase $\Delta\rho = +20\%$ and single-step Arrhenius kinetics with $E_a = 20$, $Q = 50$ and $\gamma = 1.2$: (a) The x-t diagrams showing the density contour with various wave features; (b) history of the leading shock pressure p_+/p_0 as a function of the leading shock position x_s normalized by the 90%-reaction-zone length δ.

ature decreases more while maintained the same pressure at the interface. The shock temperature of the transmitted detonation thus decreases, i.e., lower $T_{+,t}$. Since the reaction rate is exponentially dependent upon temperature, the lower shock temperature results in a longer low-shock-pressure phase (i.e., the "dip" in shock pressure as shown in 7(b)) of the transmitted detonation for increasingly greater magnitude of density increase.

Since the activation energy E_a is nondimensionalized with respect to the temperature of the initial state upstream from the interface, while holding the value $E_a = 20$ fixed, the effective activation energy is greater due to the decrease in initial temperature downstream from the interface. A greater effective activation energy leads to more pronounced inherent instabilities of detonation. [21,22] Some oscillations can thus be observed for case with a large density increase $\Delta\rho = +30\%$ in the low-shock-pressure phase as shown in Fig. 7(b).

3.3.3 Effect of reaction kinetics

The effect of different reaction kinetics on the transient process has also been explored, specifically the addition of an induction zone, by repeating the simulations using the two-step induction-reaction kinetic model. For the case with density decrease $\Delta\rho = -25\%$, as shown in Fig. 8(a), the result of the shock pressure history

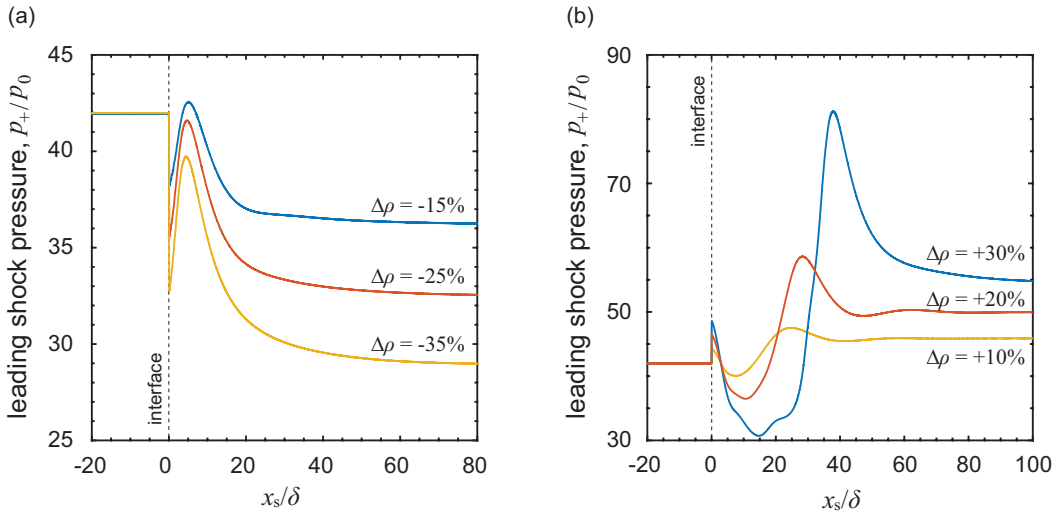

Fig. 7 History of the leading shock pressure p_+/p_0 as a function of the leading shock position x_s normalized by the 90%-reaction-zone length δ for the cases with single-step Arrhenius kinetics and various amounts of (a) density decrease and (b) density increase at the interface.

considering a two-step induction-reaction model with $\epsilon_i = 8$ and $\epsilon_r = 1$ is qualitatively similar to that obtained using single-step Arrhenius kinetics (as shown in Fig. 5(b)). Thus, the overall dynamics of the transmission process for a density-decrease interface is not qualitatively altered by considering different reaction kinetics. In order to explore the effect of the induction-reaction kinetics, the transient process that occurs immediately downstream from the interface needs to be placed under scrutiny.

In Fig. 8(b), the spatial profiles of induction progress variable ξ (blue curves) and reaction rate $\dot{\omega}$ (red curves) are plotted on an x-t diagram in a short time range during which the detonation transmits across the interface for the case with density decrease $\Delta\rho = -25\%$. Unlike with single-step kinetics, the increased shock temperature for the transmitted detonation, $T_{+,t}$ cannot immediately impact the exothermic reaction due to the presence of an induction zone. After the interface (at $t \approx 80.5$), a contact surface separates the gas that has already mostly reacted on the left from the fresh reactants at $T_{+,t}$ on the right. At this instant, the fresh shocked gas is still undergoing an induction process, i.e., has not yet begun to release energy, as $\xi < 1$. By $x/\delta \approx 0.5$ and $t \approx 81$, $\xi = 1$ is attained and reaction of the fresh gas is seen to begin in the reaction rate profiles, leading to the acceleration of the wave.

Figure 9(a) shows the change in leading shock pressure the case with $\Delta\rho = +20\%$ considering two-step induction-reaction kinetics model with $\epsilon_i = 8$ and $\epsilon_r = 1$. It is evident that the presence of the induction zone alters the transient dynamics, resulting in the failure of detonation re-initiation downstream from the interface. In Fig. 9(b), the spatial profiles of induction progress variable ξ (blue curves) and reaction rate $\dot{\omega}$ (red curves) are plotted on an x-t diagram in a short time range during which the detonation transmits across the interface for the case with density increase $\Delta\rho = +20\%$. The decreased shock temperature for the transmitted detonation results in a decrease in the induction rate $\partial\xi/\partial t$. This reduction in induction rate elongates the induction zone (as indicated in Fig. 9(b)) and causes the reaction zone to decouple from the leading shock. Unsupported by energy release, the transmitted detonation wave fails to re-initiate and eventually decays into a nonreactive shock wave.

Sets of parametric studies have then been performed to determine the critical conditions marking the limit beyond which the transmitted detonation cannot propagate in the density increase cases. The activation energy governing the induction process ϵ_i and the percentage density increase are systematically varied in these parametric studies. Figure 10 shows the histories of leading shock pressure as a function of the leading shock position for cases with $\epsilon_i = 8$, $\epsilon_r = 1$, and relatively small magnitudes of density increase at the interface. As shown in Fig. 10, for the cases with $\Delta\rho \leq 3\%$, the transmitted detonation can self-sustainably propagate; for cases with $\Delta\rho \geq 4\%$, the transmitted detonation fails to re-initiate. Hence, the critical density increase for successful transmission is determined as $\Delta\rho_{cr} = 3.5 \pm 0.5\%$ for the case with $\epsilon_i = 8$ and $\epsilon_r = 1$.

Holding $\epsilon_r = 1$ the same, the critical density increase $\Delta\rho_{cr}$ has been determined for the cases with $\epsilon_i = 5$, 6, and 7. The results of $\Delta\rho_{cr}$ (marked as black squares) are plotted on a logarithmic scale as a function of ϵ_i

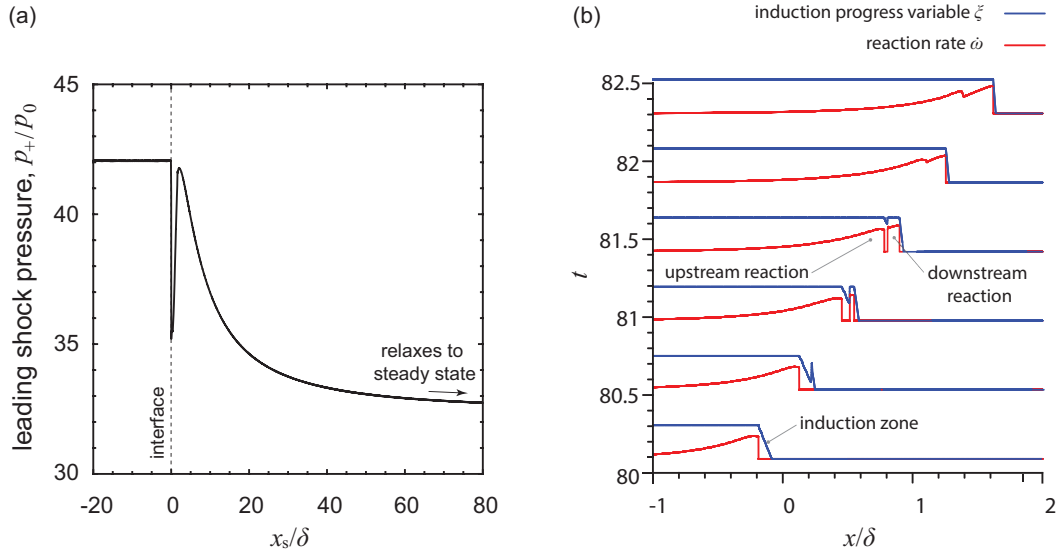

Fig. 8 Relaxation process for density decrease $\Delta\rho = -25\%$ and two-step kinetics with $\epsilon_i = 8$, $\epsilon_r = 1$, $Q = 50$, and $\gamma = 1.2$: (a) history of the leading shock pressure p_+/p_0 as a function of the leading shock position x_s normalized by the 90%-reaction-zone length δ; (b) an x-t diagram showing the profiles of induction progress variable ψ (blue curves) and reaction rate $\dot{\omega}$ (red curves) at different times as the detonation transmits across the interface.

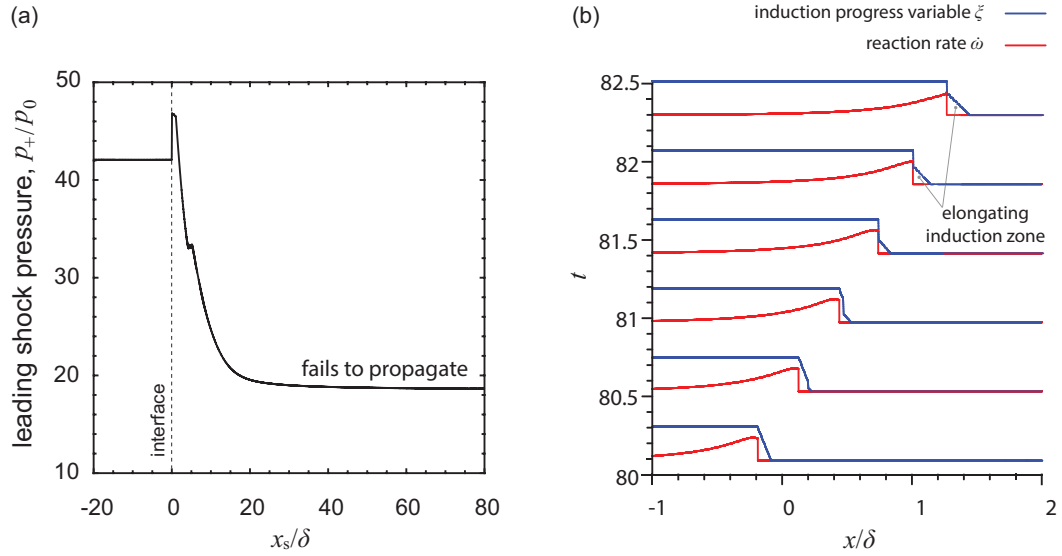

Fig. 9 Relaxation process for density increase $\Delta\rho = +20\%$ and two-step kinetics with $\epsilon_i = 8$, $\epsilon_r = 1$, $Q = 50$, and $\gamma = 1.2$: (a) history of the leading shock pressure p_+/p_0 as a function of the leading shock position x_s normalized by the 90%-reaction-zone length δ; (b) an x-t diagram showing the profiles of induction progress variable ψ (blue curves) and reaction rate $\dot{\omega}$ (red curves) at different times as the detonation transmits across the interface.

in Fig. 11. As shown in this figure, for a smaller ϵ_i, the transmitted detonation can withstand perturbation of a greater magnitude, i.e., a greater density increase at the interface. A straight line can be fitted to the data plotted on a logarithmic scale, suggesting that the activated nature of the induction kinetics is responsible for the critical behavior of the transmitted detonation.

4 Comparison of numerical and theoretical results

In the preceding section, the simulation results of the ZND-wave model show that an expansion wave is reflected from the interface for the cases with a density decrease, and a reflected shock wave for the cases with a density increase, which agree with the analytic solution of the CJ-wave model. The numerical results of the steady-state velocity of the transmitted detonations

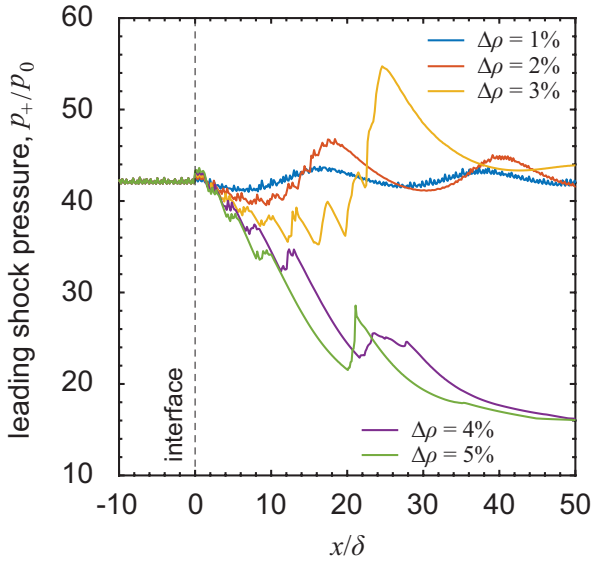

Fig. 10 History of the leading shock pressure p_+/p_0 as a function of the leading shock position x_s normalized by the 90%-reaction-zone length δ for the cases with two-step kinetics ($\epsilon_i = 8$ and $\epsilon_r = 1$) and various (relatively small) amounts of density increase.

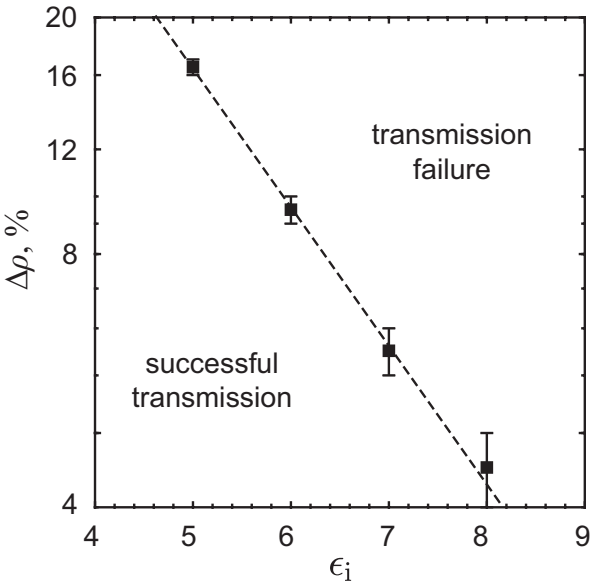

Fig. 11 The critical percentage of density increase plotted on a logarithmic scale as a function of induction-zone activation energy ϵ_i for the cases with two-step kinetics of $\epsilon_r = 1$, $Q = 50$, and $\gamma = 1.2$. The black squares are the numerical results with a fitted trendline marking the limit for the transmitted wave to propagate as a detonation.

can be compared with the corresponding theoretical results. In Fig. 12, the degree of overdrive $f = D_t^2/D_{CJ}^2$ of the transmitted detonation is plotted against percentage density change, which is varied from -35% to +30%. Note that the D_{CJ} is the CJ detonation velocity in the medium downstream from (on the right side

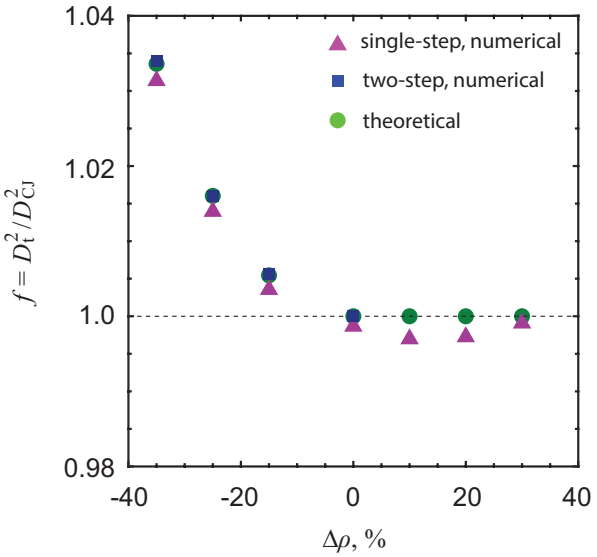

Fig. 12 Degree of overdrive f of the transmitted detonation for $\Delta\rho$ = -35% to 30%. Comparison of the numerical results and the theoretical analysis

of) the interface. The simulation results of the two reaction models (i.e., single- and two-step kinetics) are compared with the theoretical results. Only the simulation results for the two-step kinetics with $\epsilon_i = 8$ and $\epsilon_r = 1$ are plotted on Fig. 12. Thus, only the results with the single-step Arrhenius model are compared to the theoretical result for the density increase case due to the fact that the two-step kinetic model was seen to lead to failure of the transmitted detonation with a density increase greater than 3.5%, as shown in Sect. 3.3.3.

For the cases with an increase in density, the degree of overdrive is unity $f = 1$, indicating a transmitted CJ detonation. For the cases with a decrease in density, the degree of overdrive is greater than unity, i.e., $f > 1$, indicating a transmitted strong detonation. Degree of overdrive f increases with increasingly greater magnitude of $\Delta\rho$. Numerical results for both single- and two-step models are seen to agree with the theoretical predictions within 0.3%. This agreement suggests that the steady-state propagation velocity of a successfully transmitted detonation can be predicted knowing the properties of the incident detonation and the initial mixtures on both sides of the interface, independent of the detailed chemical kinetics and the relaxation dynamics. The critical conditions determining whether detonations can withstand the perturbation at the interface and successfully transmit, however, depend on the nature of the chemical kinetics.

5 Conclusion

The transmission of a detonation wave across an interface with a change in acoustic impedance has been studied analytically and computationally. Knowing the strength of the incident detonation wave and the properties in the media on both sides of the interface, the properties of the reflected wave and the transmitted detonation wave can be solved analytically, without considering the detailed reaction-zone structure. The analytic results have demonstrated that, for the cases with a density decrease (thus, a decrease in acoustic impedance) at the interface, a transmitted strong detonation and a reflected rarefaction wave are formed; for the cases with a density increase (i.e., an increase in acoustic impedance), a transmitted CJ detonation followed by an expansion fan and a reflected shock wave are formed. Thus, the transmitted detonation can be the CJ detonation solution or an overdriven strong detonation depending on the nature of the property mismatch at the interface.

This transmission problem has been investigated computationally considering an incident detonation wave with the ZND reaction-zone structure so that the transient relaxation process of the transmitted wave was has been captured. For the cases with a density decrease, the overall behavior of the relaxation process is qualitatively similar for both single-step Arrhenius kinetics and two-step induction-reaction kinetics. For the cases with a density increase and two-step kinetics, if the magnitude of the density increase is greater than a critical value, the transmitted wave fails to propagate as a self-sustainable detonation.

For the cases wherein the transmitted wave relaxes to a steady-state detonation, the simulation results of the final propagation velocity agree with the theoretical solutions. This agreement suggests that, if a detonation wave can successfully propagate after the transmission, the transient relaxation process and the reaction kinetics have no effect on the final propagation of the transmitted wave. The reaction-zone dynamics responding to the perturbation exerted by the abrupt change in acoustic impedance at the interface however determines whether the transmitted wave can eventually evolve to a steady detonation in the downstream medium.

Appendix: Analytic solutions of the CJ-wave model

Density decrease

The solution for the case with a density decrease across the interface consists of a transmitted strong detonation and a reflected expansion wave. This wave configuration corresponds to Case 2 in Table 1 and is depicted in Fig. 3(b). The initial properties at 0, 1, and 2 are known. Equations 3 and 4 are used to relate the states in front of and behind the transmitted detonation (1 and 4):

$$\begin{aligned} \frac{p_4}{p_1} &= \frac{\eta_{D,\mathrm{t}} + \gamma(1+s)}{\eta_{D,\mathrm{t}}(1+\gamma)} \\ u_4 &= D_\mathrm{t}\left[1 - \frac{\gamma + \eta_{D,\mathrm{t}} - s}{\gamma+1}\right] \end{aligned} \tag{13}$$

with

$$\begin{aligned} D_\mathrm{t} &= \frac{c_1}{\sqrt{\eta_{D,\mathrm{t}}}} \\ s &= \sqrt{(1-\eta_{D,\mathrm{t}})^2 - K\eta_{D,\mathrm{t}}} \\ K &= 2(\gamma^2-1)\frac{Q}{\gamma p_1 v_1} \end{aligned} \tag{14}$$

where D_t is the velocity of the transmitted strong detonation.

The characteristic equations (Eq. 6) express the change across the reflected expansion wave from 2 to 3:

$$u_3 = u_2 + \frac{2c_2}{\gamma-1}\left[1 - \left(\frac{p_3}{p_2}\right)^{\frac{\gamma-1}{2\gamma}}\right] \tag{15}$$

The flow behind both transmitted and reflected waves are uniform so that $p_3 = p_\mathrm{L}$, $u_3 = u_\mathrm{L}$, $p_4 = p_\mathrm{R}$, and $u_4 = u_\mathrm{R}$. The condition of mechanical equilibrium at the advected contact surface requires that $p_3 = p_4$ and $u_3 = u_4$. The following equation can thus be derived to solve for one unknown $\eta_{D,\mathrm{t}}$, which is related to the transmitted detonation velocity D_t via Eq. 14,

$$\begin{aligned} &\frac{c_1}{\sqrt{\eta_{D,\mathrm{t}}}}\left[1 - \left(\frac{\gamma + \eta_{D,\mathrm{t}} - s}{\gamma+1}\right)\right] \\ &= u_2 + \frac{2c_2}{\gamma-1}\left[1 - \left(\frac{\eta_{D,\mathrm{t}} + \gamma(s+1)}{p_2\eta_{D,\mathrm{t}}(\gamma+1)}\right)^{\frac{\gamma-1}{2\gamma}}\right] \end{aligned} \tag{16}$$

This equation can be solved iteratively to obtain $\eta_{D,\mathrm{t}}$, and thus, the transmitted detonation velocity D_t.

Density increase

The solution for the case with a density decrease across the interface consists of a transmitted CJ detonation followed by an expansion wave and a reflected shock wave. This wave configuration corresponds to Case 2 in Table 1 and is depicted in Fig. 3. Since the transmitted detonation is of the CJ solution, the flow properties at 5 are known from Eq. 3. These properties can then be related to those behind the expansion wave (at 4) using Eq. 6:

$$u_4 = u_5 - \frac{2c_5}{\gamma-1}\left[1 - \left(\frac{p_4}{p_5}\right)^{\frac{\gamma-1}{2\gamma}}\right] \tag{17}$$

This pressure and particle velocity behind the expansion wave at 4 are equal to those on the right side of the contact surface, i.e., $p_{\mathrm{R}} = p_4$ and $u_{\mathrm{R}} = u_4$.

The normal shock relations Eq. 5 are used to relate p_3 and u_3 behind the reflected shock to those in front the shock at 2:

$$\begin{aligned} \frac{p_3}{p_2} &= \frac{2\gamma M_{\mathrm{s,r}} - (\gamma - 1)}{\gamma + 1} \\ u_3 &= u_2 - (p_3 - p_2)\left[\frac{\frac{2}{(\gamma+1)\rho_2}}{p_3 + \frac{\gamma-1}{\gamma+1}p_2}\right]^{\frac{1}{2}} \end{aligned} \tag{18}$$

where $M_{\mathrm{s,r}}$ is the Mach number of the reflected shock wave. The properties on the left of the contact surface are thus $p_L = p_3$ and $u_L = u_3$. The condition of mechanical equilibrium at the advected contact surface requires that$p_L = p_R$ and $u_L = u_R$. Thus, the following two equations can be obtained for two unknowns p_4 and u_4:

$$\begin{aligned} u_4 &= u_5 - \frac{2c_5}{\gamma - 1}\left[1 - \left(\frac{p_4}{p_5}\right)^{\frac{\gamma-1}{2\gamma}}\right] \\ u_4 &= u_2 - (p_4 - p_2)\left[\frac{\frac{2}{(\gamma+1)\rho_2}}{p_4 + \frac{\gamma-1}{\gamma+1}p_2}\right]^{\frac{1}{2}} \end{aligned} \tag{19}$$

These equations can be simultaneously solved by iteration. Once p_4 and u_4 are obtained, the properties of the transmitted detonation can then be solved via Eq. 17.

Acknowledgements The authors thank A.J. Higgins for comments and feedback on the manuscript. This work is supported by the Natural Sciences and Engineering Research Council of Canada (NSERC).

References

1. D. Bjerketvedt, O. Sonju, I. Moen, The influence of experimental condition on the reinitiation of detonation across an inert region, Progress in Astronautics and Aeronautics **106**, 109 (1986). DOI https://doi.org/10.2514/5.9781600865800.0109.0130
2. G. Thomas, P. Sutton, D. Edwards, The behavior of detonation waves at concentration gradients, Combustion and flame **84**(3-4), 312 (1991). DOI https://doi.org/10.1016/0010-2180(91)90008-Y
3. S. Boulal, P. Vidal, R. Zitoun, Experimental investigation of detonation quenching in non-uniform compositions, Combustion and Flame **172**, 222 (2016). DOI https://doi.org/10.1016/j.combustflame.2016.07.022
4. D. Lieberman, J. Shepherd, Detonation interaction with an interface, Physics of Fluids **19**(9), 096101 (2007). DOI https://doi.org/10.1063/1.2768903
5. J. Peace, F. Lu, Detonation-to-shock wave transmission at a contact discontinuity, Shock Waves pp. 1–12 (2018). DOI https://doi.org/10.1007/s00193-018-0804-6
6. R. Strehlow, R. Stiles, A. Adamczyk, Transient studies of detonation waves, Astronautica Acta **17**(4-5), 509 (1972)
7. M. Kuznetsov, V. Alekseev, S. Dorofeev, I. Matsukov, J. Boccio, Detonation propagation, decay, and reinitiation in nonuniform gaseous mixtures, Symposium (International) on Combustion **27**(2), 2241 (1998). DOI https://doi.org/10.1016/S0082-0784(98)80073-8
8. M. Kuznetsov, S. Dorofeev, A. Efimenko, V. Alekseev, W. Breitung, Experimental and numerical studies on transmission of gaseous detonation to a less sensitive mixture, Shock Waves **7**(5), 297 (1997). DOI https://doi.org/10.1007/s001930050084
9. J. Li, W. Lai, K. Chung, F. Lu, Experimental study on transmission of an overdriven detonation wave from propane/oxygen to propane/air, Combustion and Flame **154**(3), 331 (2008). DOI https://doi.org/10.1016/j.combustflame.2008.04.010
10. J. Li, K. Chung, Y. Hsu, Diaphragm effect on the detonation wave transmission across the interface between two mixtures, Combustion, Explosion, and Shock Waves **51**(6), 717 (2015). DOI https://doi.org/10.1134/S0010508215060131
11. H. Ng, B. Botros, J. Chao, J. Yang, N. Nikiforakis, J. Lee, Head-on collision of a detonation with a planar shock wave, Shock Waves **15**(5), 341 (2006). DOI https://doi.org/10.1007/s00193-006-0022-5
12. B. Botros, H. Ng, Y. Zhu, Y. Ju, J. Lee, The evolution and cellular structure of a detonation subsequent to the head-on interaction with a shock wave, Combustion and Flame **151**, 573 (2007). DOI https://doi.org/10.1016/j.combustflame.2007.07.018
13. A. Haselbacher, On impedance in shock-refraction problems, Shock Waves **22**(4), 381 (2012). DOI https://doi.org/10.1007/s00193-012-0377-8. URL https://doi.org/10.1007/s00193-012-0377-8
14. J. Lee, *The Detonation Phenomenon* (Cambridge University Press, Cambridge; New York, 2008). DOI https://doi.org/10.1017/CBO9780511754708
15. A. Higgins, Steady one-dimensional detonations, in *Shock Waves Science and Technology Library*, vol. 6, ed. by F. Zhang (Springer Berlin Heidelberg, 2012), pp. 33–105. DOI 10.1007/978-3-642-22967-1_2
16. E. Toro, *Riemann Solvers and Numerical Methods for Fluid Dynamics : A Practical Introduction* (Springer, Berlin, 2006). DOI 10.1007/978-3-662-03490-3. URL http://site.ebrary.com/id/10294547
17. H. Ng, N. Nikiforakis, J. Lee, Assessment of a high resolution centered scheme for detonation modelling. Technical report (2000)
18. H. Ng, M. Radulescu, A. Higgins, N. Nikiforakis, J. Lee, Numerical investigation of the instability for one-dimensional chapman–jouguet detonations with chain-branching kinetics, Combustion Theory and Modelling **9**(3), 385 (2005). DOI https://doi.org/10.1080/13647830500307758
19. A. Hindmarsh, K. Radhakrishnan, Description and use of lsode, the livermore solver for ordinary differential equations. Tech. Rep. UCRL-ID-113855 (1993)
20. I. Glass, J. Sislian, *Nonstationary Flows and Shock Waves*. Oxford Engineering Science Series (Clarendon Press, 1994). URL https://books.google.ca/books?id=DpIeAQAAIAAJ
21. H. Lee, D. Stewart, Calculation of linear detonation instability: one-dimensional instability of plane detonation, Journal of Fluid Mechanics **216**, 103 (1990). DOI https://doi.org/10.1017/S0022112090000362

22. H. Ng, F. Zhang, Detonation instability, in *Shock Waves Science and Technology Library*, vol. 6 (Springer Berlin Heidelberg, 2012), pp. 107–212. DOI 10.1007/978-3-642-22967-1_3